

Zooplankton target strength: Volumetric or areal dependence?

David A. Demer

Scripps Institution of Oceanography, University of California at San Diego, La Jolla, California 92038-0203

Linda V. Martin

Woods Hole Oceanographic Institution, Woods Hole, Massachusetts 02543

(Received 11 July 1994; revised 22 December 1994; accepted 6 February 1995)

Target strengths (TS) of various zooplankton were measured at 200 kHz, 420 kHz, and 1 MHz and the dependence of these data on animal volume versus cross-sectional area was explored. The 420-kHz and 1-MHz data were collected with a dual-beam sonar system and the 200-kHz data with a split-beam system. Experiments were conducted with live, tethered individuals in an enclosure filled with filtered seawater. The data were compared to both empirical and theoretical models of reduced target strength (TS normalized by the square of the animal length) versus ka (the product of wave number and equivalent cylindrical radius). The theoretical models chosen for this comparison were two versions of a high-pass bent-cylinder model (Stanton, 1989b) that indicate TS is dependent on animal volume, and the ray bent-cylinder model (Stanton, 1993a) which implies TS is dependent on the cross-sectional area. The dependence of acoustic backscattering on animal volume or area was tested by fitting regression lines for TS versus the logs of ka , length (L), wet weight (WW), and dry weight (DW). Contrary to an empirical model derived from similar experiments (Wiebe *et al.*, 1990), and to the high-pass models, the regressions indicated that TS is proportional to the cross-sectional area of the animal. However, because scattering from individual zooplankton is highly nonlinear, especially in the geometric scattering region ($ka > 1$), linear regressions of TS versus the log of ka , L , WW, or DW can be misleading. Furthermore, neither Wiebe *et al.* (1990) nor this experiment directly accounted for animal orientations. Simulations using a distorted-wave Born-approximation model (Chu *et al.*, 1993), indicated that animal behavior is an important factor in the scattering characteristics of zooplankton. Different distributions of animal tilt angle can influence the general trend of the TS model to exhibit either areal or near volumetric dependence. © 1995 Acoustical Society of America.

PACS numbers: 43.30.Pc, 43.30.Ft, 43.30.Sf

INTRODUCTION

Many experimental and theoretical studies have been conducted to characterize the acoustic target strength (TS) of zooplankton for the purposes of species identification, acoustic signal separation, and abundance estimation (e.g., Anderson, 1950; Greenlaw, 1979; Richter, 1985; Holliday *et al.*, 1989; Foote *et al.*, 1990; Wiebe *et al.*, 1990; Chu *et al.*, 1993). The echo integration method for acoustic biomass estimation relies on an accurate knowledge of the species of scatterers in the insonified volume and their respective scattering characteristics (Stanton *et al.*, 1994). This understanding is necessary to convert integrated backscattered energy to numerical densities and apportion these densities to individual species. Complicating this translation is the variance in sound scattering introduced by differences in animal size, shape, acoustic impedance, and orientation (Stanton, 1989a; Foote *et al.*, 1992).

Various models have been developed to predict the scattering from elongated zooplankton. Some of these models imply that TS is dependent on the cross-sectional area of the animal (Anderson, 1950; Greenlaw, 1977, 1979; Chu *et al.*, 1993; Stanton *et al.*, 1993a, b), and others indicate that TS is primarily affected by the animal's volume (Richter, 1985; Stanton, 1989a, b; Wiebe *et al.*, 1990; Greene *et al.*, 1991).

A scattering model is considered to be dependent on the animal's volume (V) if plots of TS as a function of the log of ka [the product of the acoustic wave number (k) and the equivalent cylindrical or spherical radius of the animal (a)] and TS versus the log of animal length (L) have slopes of 30 in the geometric scattering region ($ka > 1$) (Wiebe *et al.*, 1990). These gradients are indicative of the proportional relationship of TS to L^3 :

$$TS \propto 10 \log(V) \propto 30 \log(L). \quad (1)$$

If V is proportional to the wet weights (WW) and dry weights (DW) of the animals, the slopes of the TS versus the log of weight curves will be 10:

$$TS \propto 10 \log(WW) \propto 10 \log(DW). \quad (2)$$

Likewise, for a scattering model to be dependent on the cross-sectional area (A) of an animal, the slope of the TS versus the log of ka and L functions must be 20 in the geometric scattering region (Wiebe *et al.*, 1990). This slope is indicative of the proportionality between A and L^2 :

$$TS \propto 10 \log(A) \propto 20 \log(L). \quad (3)$$

Since $V \propto L^3$ and $A \propto L^2$,

$$A \propto V^{2/3}. \quad (4)$$

Therefore for scattering to be dependent on A , the slope of TS versus the log of WW and DW curves should be $20/3$ (≈ 6.7) in the geometric scattering region:

$$TS \propto \frac{20}{3} \log(WW) \propto \frac{20}{3} \log(DW). \quad (5)$$

It is important to note, however, that scattering from elongated zooplankton as a function of acoustic frequency and animal size is highly nonlinear in the geometric region (Chu *et al.*, 1992). Thus the linear relationships described above are fictive but have been used to describe the general trends of the scattering functions. Wiebe *et al.* (1990) used linear regression analysis as a "first approximation" to an otherwise very complex problem.

To develop and corroborate scattering models, TS measurements have been made of zooplankton, both experimentally constrained and *in situ* (Foote, 1991). Wiebe *et al.* (1990) used TS measurements of experimentally constrained crustacean zooplankton and micronekton to derive an empirical, volume-dependent, TS model and to corroborate high-pass cylinder models (Stanton, 1989b) which were also dependent on V . Greene *et al.* (1991) adapted the empirical model to predict scattering from Antarctic krill (*Euphausia superba*) for a wide range of frequencies and animal lengths. Hewitt and Demer (1991) recorded *in situ* TS measurements of Antarctic krill at 120 kHz which were in accordance with predictions from the Greene *et al.* empirical model. Foote *et al.* (1990) insonified live aggregations of *E. superba* in a cage at 38 and 120 kHz and compared the data to predictions of an areally dependent fluid sphere model (Greenlaw, 1979). Chu *et al.* (1993) used the data from Foote *et al.* (1990) to demonstrate a better fit to an areally dependent bent-cylinder model. It is therefore uncertain whether elongated zooplankton scatter sound as a function of their volume or their cross-sectional area. This paper is an investigation of these apparently contradictory models.

Acoustic backscatter of various zooplankton were measured at 200 kHz, 420 kHz, and 1 MHz. The species insonified included several elongated crustaceans such as ghost shrimp (*Neomysis kadiakensis*), kelp shrimp (*Heptacarpus stylus*), and calanoid copepods (*Neocalanus cristatus*). The data were used to test the validity of empirical and theoretical models of TS vs ka . The effects of varying model parameters (distribution of tilt angle) were investigated to determine if different simplified models may be suitable under different circumstances. Moreover, the validity of linear regression analyses to determine volumetric or areal dependence of TS is examined.

I. METHODS

Experiments were conducted at Friday Harbor Laboratories (FHL), Friday Harbor, WA from 10–14 August, 1993. Two echo sounders were used for all of the experiments: a split-beam system configured with a 200-kHz transducer and a dual-beam system configured with a 420-kHz and a 1-MHz transducer. System calibrations were performed before and after the series of experiments. TS data were measured from individual live animals suspended in a cylindrical enclosure which was deployed off of a dock at FHL (Fig. 1). To enhance the accuracy and precision of the TS distributions, data

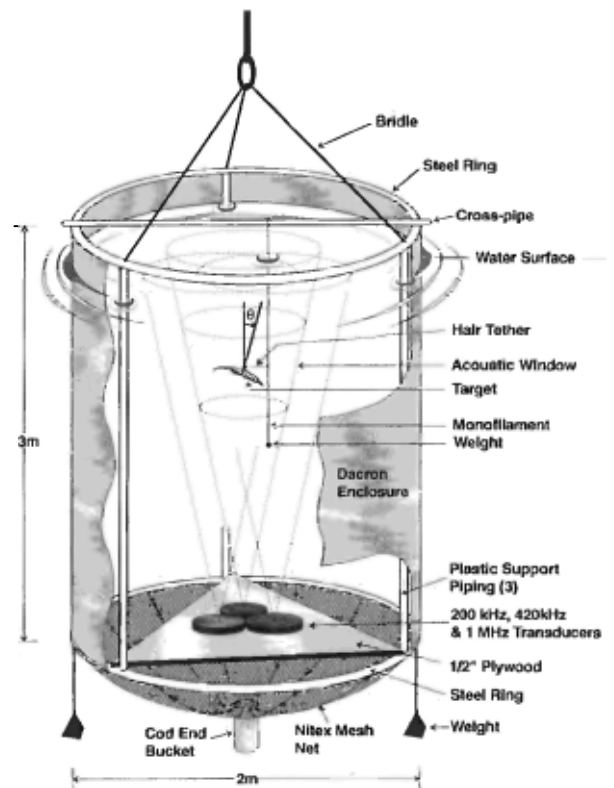


FIG. 1. The experimental enclosure was the same one used in Wiebe *et al.* (1990). It was cylindrical and 3 m deep by 2 m in diameter. The sides were constructed with black Dacron cloth and the bottom with 53- μ m mesh. Three transducers (200 kHz, 420 kHz, and 1 MHz) were mounted on the bottom of the tank in an upward looking configuration. Individual zooplankton were suspended in the acoustic beams at a range of 1.8–2.2 m via monofilament line and human hair.

were filtered by range, time, and angle off-axis. L , WW, and DW were measured for each of the animals immediately following the TS measurements.

The 200-kHz split-beam transducer had a narrow-beam pattern with 6° between half-power points. A 0.4-ms pulse was transmitted on four transducer quadrants every 0.1 s. Phase differences between the signals received at each of the four quadrants were used to determine the location of the target in the beam. The 420-kHz and 1-MHz dual-beam transducers were comprised of both narrow- (3°) and wide-beam (16°) elements. A 0.3-ms pulse was transmitted every 0.1 s on the narrow-beam transducer elements and received on both the narrow-beam and a wide-beam transducer elements. The differences in echo intensities received by the narrow- and wide-beam elements were used to determine the off-axis angle of the target. On both systems, measurements of the backscattering cross-sectional area (σ_{ba}) were then corrected by removing the circularly symmetric beam pattern effects.

Calibration of the split-beam system was performed in a test tank on 9 August 1993. The water temperature was 20.6°C and the separation between the system transducer and the standard transducer was 5.4 m. Measurements included source level, receiver sensitivity, receiver beam pattern, and angle sensitivity (the relationship between the electrical phase and mechanical off-axis angles).

TABLE I. Summary of zooplankton lengths (L), wet weights (WW), dry weights (DW), mean target strengths (\overline{TS}), number of observations (n), reduced mean target strengths ($RTS = \overline{TS} - 20 \log L$), and the equivalent cylindrical radius times wave number [ka , where $a = (V/\pi L)^{1/2}$ and $V = WW/10^4$]. Data are tabulated in order of ascending ka . Because the calibration methods were different both pre- and postexperiment and for the two echosounders, the reader should not consider these \overline{TS} values as absolute measurements.

Run	Species name	L mm	WW mg	DW mg	200 kHz				420 kHz				1 MHz			
					\overline{TS}	n	RTS	ka	\overline{TS}	n	RTS	ka	\overline{TS}	n	RTS	ka
8	<i>Neocalanus cristatus</i>	7.0	7.3	0.9	-75.0	45	-31.9	0.49	-81.7	9	-38.6	1.03				
23	<i>Neocalanus cristatus</i>	7.1	8.1	1.0					-87.9	34	-44.8	1.08	-74.6	319	-31.6	2.56
24	<i>Neocalanus cristatus</i>	6.7	8.5	1.1					-89.0	192	-45.5	1.14	-77.7	348	-34.2	2.72
10	<i>Melita dentata</i>	8.8	12.5	3.9	-73.8	198	-32.7	0.57	-78.4	265	-37.3	1.21				
9	<i>Neomysis kadiakensis</i>	18.5	29.9	5.8	-77.1	762	-42.5	0.61	-79.4	68	-44.7	1.29	-76.8	67	-42.1	3.07
6	<i>Neomysis kadiakensis</i>	15.2	28.2	5.9	-76.9	578	-40.5	0.66	-77.2	58	-40.8	1.38				
12	<i>Neomysis kadiakensis</i>	20.0	47.6	9.2	-76.2	463	-42.3	0.74	-78.5	169	-44.5	1.56				
16	<i>Heptacarpus stylus</i>	14.6	38.8	9.1	-74.1	1854	-37.4	0.79	-82.9	246	-46.2	1.65	-68.2	1060	-31.5	3.93
18	<i>Heptacarpus stylus</i>	16.8	51.6	11.8	-82.9	607	-47.4	0.85	-79.8	229	-44.3	1.78	-67.1	744	-31.6	4.23
11	<i>Crangon alba</i>	15.1	46.5	12.3	-60.4	3494	-24.0	0.85	69.1	149	-32.7	1.78	-74.5	121	-38.1	4.23
7	<i>Neomysis kadiakensis</i>	25.8	99.9	19.5	-76.6	377	-44.9	0.95	-79.0	304	-47.2	1.99				
17	<i>Heptacarpus stylus</i>	20.2	80.1	19.5	-80.7	476	-46.8	0.96	-75.6	657	-41.7	2.02	-69.5	715	-35.6	4.80
19	<i>Heptacarpus stylus</i>	26.8	216.5	54.9	-83.1	995	-51.6	1.37	79.9	492	-48.5	2.88	-70.1	541	-38.7	6.85
21	<i>Heptacarpus stylus</i>	33.0	436.6	104.8	77.9	967	-48.2	1.75	-74.7	493	-45.0	3.68	-66.5	530	-36.9	8.77
20	<i>Heptacarpus stylus</i>	34.8	500.2	127.6	-71.9	787	-42.7	1.83	73.1	642	-43.9	3.84	-61.2	820	-32.0	9.14
15	<i>Heptacarpus stylus</i>	35.2	611.4	153.6	-63.4	1508	-34.3	2.01	-78.3	1225	-49.2	4.22	-67.4	684	-38.3	10.05
14	<i>Heptacarpus stylus</i>	37.6	691.9	147.8	-69.2	1536	-40.7	2.07	-75.7	519	-47.2	4.34	-64.5	429	-36.0	10.34
3	<i>Pandalus danai</i>	49.0	2161.9	509.2					-80.0	277	-53.8	6.73				
1	<i>Pandalus danai</i>	57.0	3479.5	676.6					-71.6	502	-46.7	7.91				

The dual-beam systems were pre- and postcalibrated in a test tank on 27 July and 10 September 1993. The water temperature was 21.0 °C and the separation between the system transducers and the standard transducers was 1.2 m. Measurements included source levels, receiver sensitivities, and receiver beam patterns. Postcalibration results for the 420-kHz sounder indicated that the off-axis compensation may have been in error. The effects of this possible bias were effectively avoided by filtering the data to include only the measurements made within 1.5° of the beam axis.

The cylindrical enclosure was 3 m deep and 2 m in diameter (Fig. 1). The sides were constructed with black Dacron cloth and the bottom with 53- μ m mesh. Support was provided at the top and bottom with stainless-steel (SS) rings and on the sides with three polyvinyl-chloride pipes (2.5 cm diameter by 3 m long). The enclosure was suspended from a SS bridle at the top and ballasted from the bottom by three weights of approximately 10 kg each. A triangular piece of plywood was used to mount the three transducers around the center of the tank in an upward looking configuration. To position the individual zooplankton in the acoustic beams, a metal pipe was fixed across the center of the upper SS ring and a weight was suspended from this pipe via a 10- μ m-diameter monofilament line. The individual animals were then tethered to the monofilament line via a human hair at a range of 1.8–2.2 m from the transducers. The zooplankton specimens were collected around FHL with a 1-m hoop net with a hard cod end.

TS measurements of the individual animals were recorded in succession. The 200-kHz split-beam system transmitted asynchronously, but concurrently, with the dual-beam system. However, since the dual-beam system was limited to single frequency operation, the TS measurements at 420 kHz and 1 MHz were recorded in turn. TS data were filtered by

narrow range gates around the targets (0.2 m), and by time spans of low noise. Additionally, the data were limited to echoes determined to originate from within the half-power points of the narrow beams. L and WW data were recorded immediately following the acoustic measurements. DW data were recorded after drying to equilibrium at approximately 60 °C (Table I).

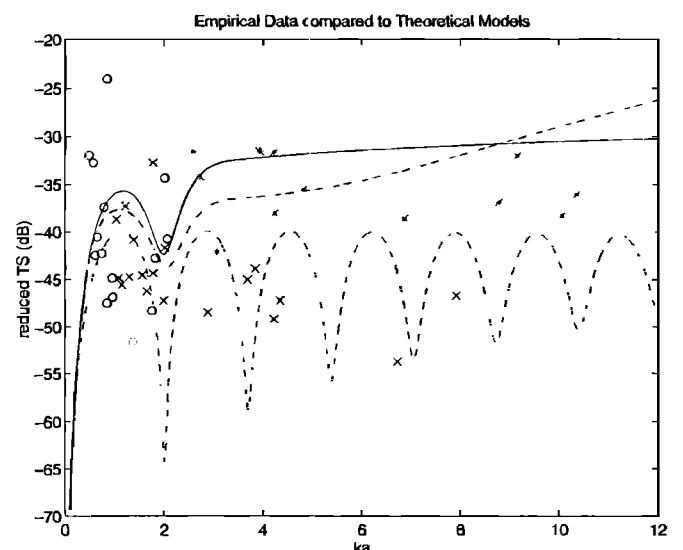


FIG. 2. Experimental data compared to predictions of the HPBC I (---), the HPBC II (-.-) and the ray BC (—) models. Each data point represents the average reduced TS of one animal at 200 kHz (O), 420 kHz (X), and 1 MHz (*). Following Foote (1990) and Wiebe *et al.* (1990) for the HPBC models: $g = 1.0357$ and $h = 1.0279$. Parameters for the ray BC were chosen as per Stanton *et al.* (1993b): $g = h = 1.06$, θ distributed uniformly, and s (standard deviation of L divided by L) = 0.015. L was $10.5 \times a$ for all models.

TABLE II. Linear regression summary. Slopes were derived for the empirically measured TS data versus the logs of ka , animal length (L), wet weight (WW), and dry weight (DW); correlation coefficient in parentheses. The regression results were compared to data from a similar experiment by Wiebe *et al.* (1990) which were measured at 420 kHz. Following Wiebe *et al.*, ka is the wave number times the equivalent spherical radius [$a=(V/\pi)^{1/3}$, where $V=WW/10^4$].

TS vs:	200 kHz	420 kHz	1 MHz	Wiebe <i>et al.</i> (1990)	HPBC ^a	Ray BC ^b
ka	30.90(.20)	18.05(.56)	21.98(.82)	30.84(.89)	30	20
L	29.51(.10)	17.32(.62)	19.78(.78)	31.11(.85)	30	20
WW	10.30(.20)	6.02(.56)	7.33(.82)	10.27(.89)	10	~6.7
DW	9.65(.21)	5.62(.61)	6.55(.82)	9.68(.91)	10	~6.7

^aDependent on volume.

^bDependent on cross-sectional area.

TS data were measured for 20 different animals at one or more of the three frequencies. Average values for each individual at each frequency were compared to predictions from three theoretical models of TS vs ka (Fig. 2). The models, appropriate for elongated, fluidlike, cylindrical zooplankton, include two versions of Stanton's (1989b) high-pass bent-cylinder model (HPBC I and HPBC II) and the ray bent-cylinder model (ray BC) (Stanton *et al.*, 1993a). HPBC I is the truncated modal series solution and HPBC II is a version based on data from preserved euphausiids. Ray BC represents the converged solution for scattering from a deformed cylinder. Following Stanton *et al.* (1993b), the model was averaged over tilt angle (θ) measured from broadside incidence and L .

Least-squares linear (functional) regression analyses were performed on the experimentally measured TS data versus the logs of ka , L , WW, and DW (Table II). The regression slopes are compared to the results of a similar experiment (Wiebe *et al.*, 1990). Comparisons are made for each individual frequency. Because much of the 200-kHz data was in the Rayleigh scattering region, the three frequencies were not combined for this analyses.

Live marine animals assume a variety of orientations which can be partially described by their tilt angle (θ) (Fig. 1). This behavior has been shown to have a dominant influence on the scattering properties of elongated animals (Stanton, 1989a). The effect of this behavior on the scattering properties of zooplankton can be investigated through a deformed cylinder model evaluated by the distorted-wave Born approximation (DWBA) (Chu *et al.*, 1993). Assuming a normal distribution of orientations (N), this model provides absolute predictions of TS at each frequency.

Several simulations were performed using the DWBA over a large range of ka (0.5–11). The behavior of the animal was parameterized by its mean orientation angle (μ_θ),

measured from broadside incidence, and the standard deviation of this angle (σ_θ). For comparison with the empirical TS data, linear regressions of 20 predicted TS values [DWBA with $N(\mu_\theta, \sigma_\theta)$] versus linearly spaced ka yielded the slopes shown in Table III.

Because scattering from individual zooplankton is oscillatory in the geometric scattering region (Fig. 3), the linear regression analyses are highly dependent on the range and spacing of ka 's. To investigate this dependence, a Monte Carlo simulation was performed to define the expected distributions of slopes which could result from variations in the range of ka ($0 \leq ka \leq 10$, $1 \leq ka \leq 11$, and $5 \leq ka \leq 15$) and the number of data points ($n=20$ and 100). A matrix of six simulations were run using the ray BC model, averaged over θ (Stanton, 1993b) (Fig. 4). At 420 kHz, the range of ka 's from 1 to 11 matches the size distribution of animals in this experiment and in Wiebe *et al.* (1990) (assuming $a=L/10.5$). Ensembles of 20 and 100 TS values were calculated at ka 's which were randomly generated from a uniform distribution. The slopes of 10 000 TS ensembles versus $\log(ka)$ were calculated by least-squares linear regression for each combination of n and range of ka (see Table IV). Each set of slope-frequency data was normalized by the number of ensembles to create a probability density function (PDF) (Fig. 4). Using chi-square tests, the resulting PDFs were shown to be statistically indistinguishable from normal distributions with mean slopes (μ_s) and standard deviations (σ_s).

The effects of target behavior on the slopes of linear regressions can be confounded by the effects of the spacing and range of ka 's chosen for the regression. To isolate the behavioral effect, the general slope of the DWBA model was reevaluated under conditions of different orientation distributions [$N(\mu_\theta, \sigma_\theta)$]. For each distribution, the DWBA model was used to generate 1000 points ($0.5 \leq ka \leq 11$). In the portion of the geometric scattering region ($1 \leq ka \leq 11$) the

TABLE III. Summary of DWBA simulations for a variety of normally distributed tilt angles [$N(\mu_\theta, \sigma_\theta)$]. Parameters for the DWBA model were set as per Chu *et al.* (1993). Values for each mean tilt angle (μ_θ) and standard deviation (σ_θ) are the slopes of linear regressions of 20 TS data vs their respective $\log(ka)$ values (linearly spaced from 0.5 to 11). Ellipses (...) depict combinations of μ_θ and σ_θ which were not included in this analysis.

μ_θ/σ_θ	2	4	6	8	10	20	40	60
0	25.3	25.3	24.7	24.2	23.7	22.6	21.8	21.5
20	20.3	22.0	21.7	21.5
40	19.8	20.0	21.4	21.3
60	21.3	21.0	21.0	21.2
80	28.2	26.7	25.5	24.8	24.3	22.7	20.6	21.2

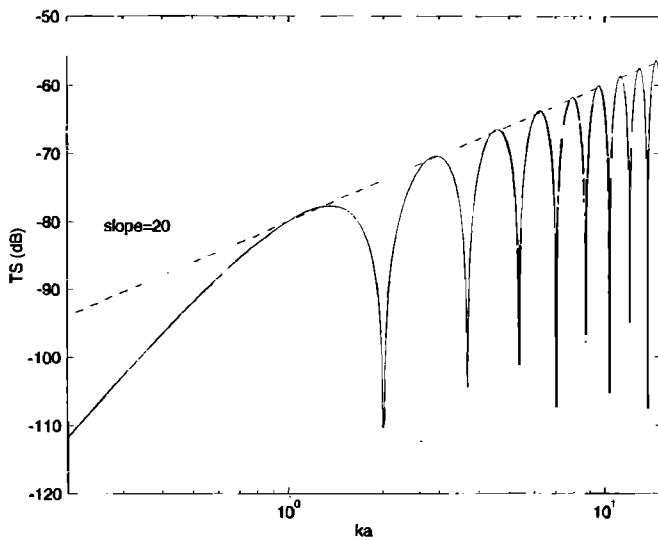


FIG. 3. The ray BC model averaged over L and plotted for 420 kHz (-). Parameters were $g=h=1.06$, θ distributed uniformly, and $a=L/10.5$. The peaks of the model indicate areal dependence because the tangent line (--) has a slope=20.

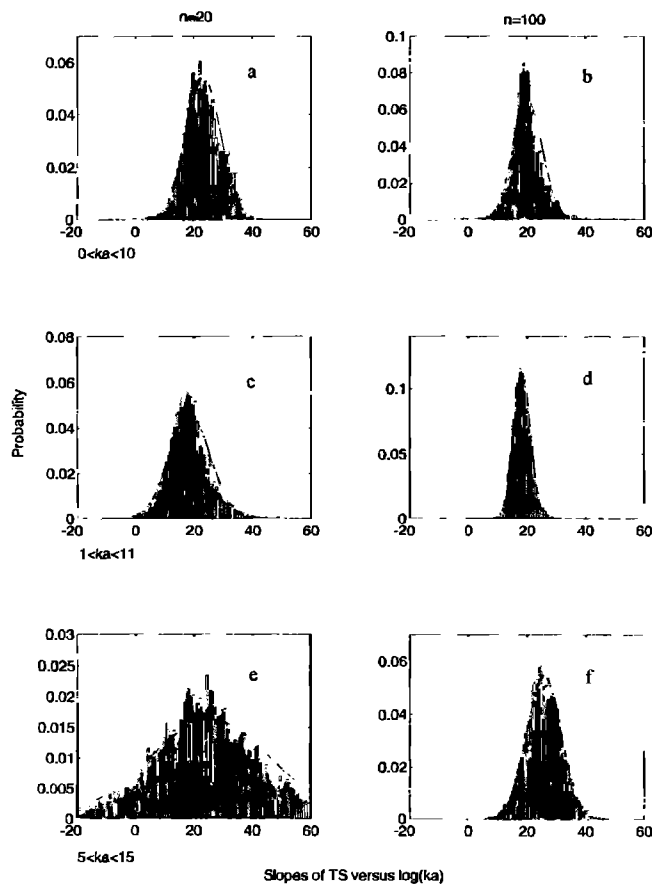


FIG. 4. Monte Carlo simulation results showing the PDFs of slopes of TS vs $\log ka$. The simulations of 10 000 slopes for each combination of n (20 and 100 TS/ ka pairs per regression) and range of ka ($0 \leq ka \leq 10$, $1 \leq ka \leq 11$, and $5 \leq ka \leq 15$) yielded normal distributions. Because scattering from individual zooplankton is oscillatory, the linear regression analyses can result in either areal or volumetric dependence (95% confidence level) dependent only on the range and spacing of ka 's.

TABLE IV. Summary of the Monte Carlo simulations for slopes of TS vs $\log(ka)$. The largest mean slopes (μ_s) were generated for the high ka range because of the reduced spacing between nulls [Fig. 4(e) and (f)]. Intermediate values resulted from the lowest range of ka 's due to the inclusion of the Rayleigh scattering region [Fig. 4(a) and (b)]. The lowest mean slopes were generated for the intermediate range of ka [Fig. 4(c) and (d)]. The standard deviation of the slopes (σ_s) decreased nonlinearly with an increase in the number of data points (n) in the regression.

ka range	μ_s/σ_s	
	$n=20$	$n=1000$
$0 \leq ka \leq 10$	23.06/6.02	20.25/4.93
$1 \leq ka \leq 11$	18.53/7.18	18.32/2.91
$5 \leq ka \leq 15$	25.16/21.02	25.76/5.95

slopes of tangent lines between successive peaks of the functions were either constant or monotonically decreasing (Fig. 5). Therefore the slopes of two tangent lines (between the first two and the last two peaks) were used to define the range of slopes for each behavior in the absence of ka -spacing effects (Table V).

II. RESULTS

The approximate models (HPBC I and HPBC II) do not predict the experimental TS data nearly as well as the converged solution (ray BC), particularly in the geometric scattering range (Fig. 2). The large variance of the TS data is likely due to the nonlinearity of zooplankton TS vs ka (Chu *et al.*, 1992). The deep nulls in the ray BC and DWBA models are therefore supported by these data as well as by Chu *et al.* (1993) and Demer and Hewitt (submitted).

The results of the regression analyses of the experimental data suggest that TS is dependent on the cross-sectional area of the animal (Table II). This result is in accordance with the ray BC model which also predicts that TS is, in general, proportional to the cylindrical cross section in the geometric scattering region. In contrast, Wiebe *et al.* (1990) found TS to be dependent on the volume of the target.

Apparent inconsistencies between the results of this experiment and those of Wiebe *et al.* (1990) may be partially explained by the effect of animal behavior. Simulations using the DWBA model and various distributions of θ produced regression slopes which indicated either areal or volumetric dependence (Table III). The tilt angle and the standard deviation of θ affected the estimated slopes. For animals oriented to broadside incidence ($\mu_\theta=0$), regression slopes ranged from 21.5 to 25.3 depending on σ_θ . For near-end-on incidence ($\mu_\theta=80$), slopes ranged from 21.2 to 28.2. In short, these results imply that differences in animal behavior can lead to linear regression results which indicate either volumetric or areal dependence of TS.

The simulations of 10 000 slopes [TS vs $\log(ka)$] for each combination of n and range of ka yielded normal distributions with mean slopes (μ_s) ranging from 18.32 to 25.76 and standard deviations (σ_s) ranging from 2.91 to 21.02 (Fig. 4). The largest mean slopes were generated for the high ka range ($5 \leq ka \leq 15$) because of the reduced spacing between nulls and the corresponding increase in probability that the data will fall in a null [Fig. 4(e) and (f)]. Intermediate mean

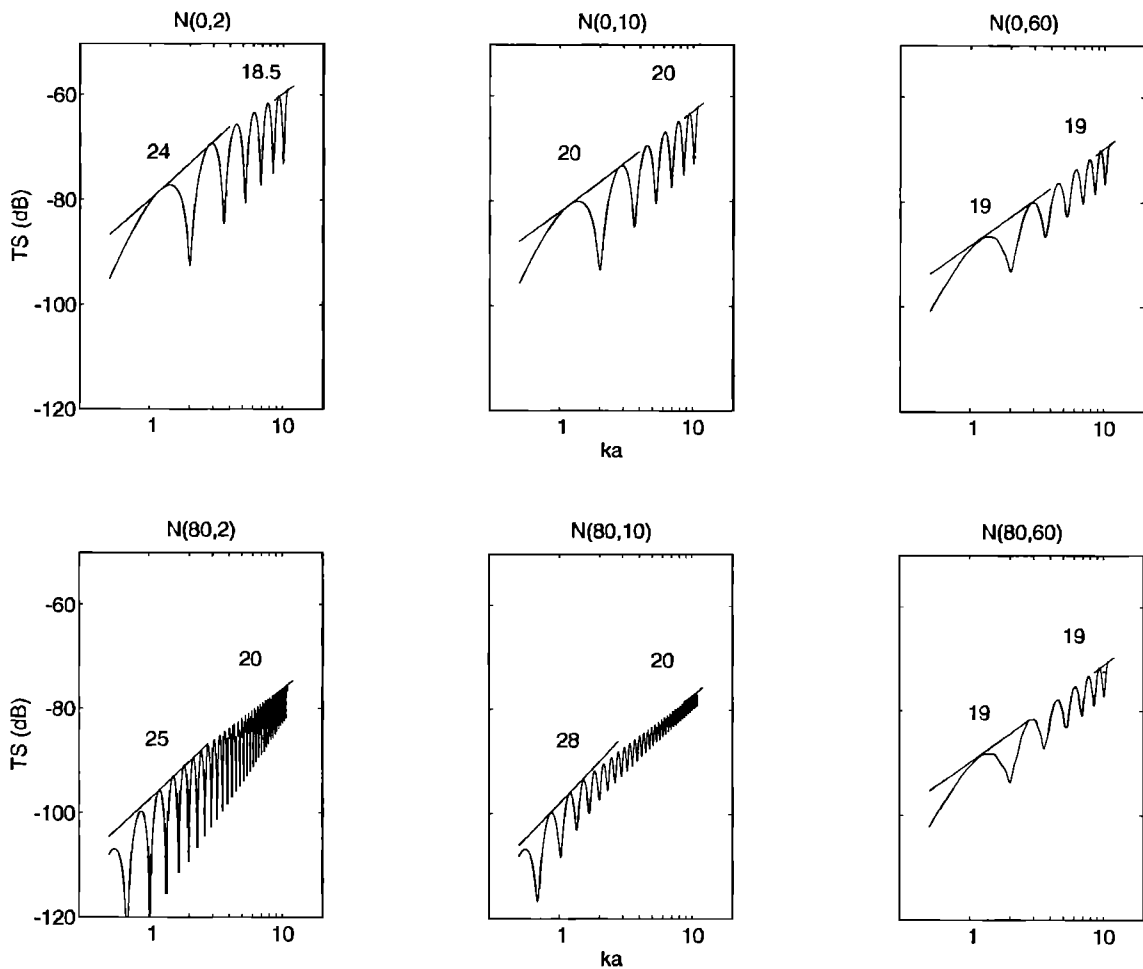


FIG. 5. Animal behavior as modeled by normally distributed tilt angles [$N(\mu_\theta, \sigma_\theta)$] and the distorted-wave Born-approximation model. For each mean tilt angle (μ_θ) and standard deviation (σ_θ), 1000 TS data were generated for ka 's between 0.5 and 11. The general trends of the DWBA curves were parameterized by the maximum and minimum slopes of tangent lines fit between the first two and last two peaks. These graphs are a subset of the complete matrix of simulations summarized in Table V.

slopes resulted from the lowest range of ka 's ($0 \leq ka \leq 10$), due to the inclusion of the Rayleigh scattering region [Fig. 4(a) and (b)]. The lowest mean slopes were generated for the intermediate range of ka [Fig. 4(c) and (d)]. For all ranges of ka , the variances decreased nonlinearly as the ensembles were increased from $n=20$ to 100. Depending on the range and values of ka 's, the proportionality constants between TS and $\log(ka)$ ranged from about -30 to 70 [Fig. 4(e)].

Of particular importance is the combination of $n=20$

and $1 \leq ka \leq 11$ [Fig. 4(c)], which corresponds to the conditions of the experimental data as well as the range of ka 's in Wiebe *et al.* (1990); the PDF has a mean slope of 18.53 and a standard deviation of 7.18. This means that if scattering from zooplankton is predictable by an areally dependent ray BC model, linear regression analyses may lead to the erroneous conclusion (95% confidence level) that TS is volumetrically dependent.

For the behavioral simulations centered on broadside in-

TABLE V. Summary of the second set of DWBA simulations for a variety of normally distributed tilt angles [$N(\mu_\theta, \sigma_\theta)$], unconfounded by ka spacing. For each mean tilt angle (μ_θ) and standard deviation (σ_θ), the DWBA model was used to generate 1000 TS data corresponding to ka 's between 0.5 and 11. Tabulated values are the slopes, or ranges of slopes, of tangent lines to the successive peaks of the modeled functions. Ellipses (...) depict combinations of μ_θ and σ_θ which were not included in this analysis. Note that the DWBA model breaks down near end-on incidence ($\theta=90$) (Chu *et al.*, 1993) and wide distributions around $\mu_\theta=80$ may include this value of θ .

$\mu_\theta \backslash \sigma_\theta$	2	4	6	8	10	20	40	60
0	18.5-24	20-21.5	20-21	20	20	19.5	19	19
20	18	19	19	19
40	16-20	18	19	19
60	20-22	19-20	19	19
80	20-25	17-25	17-25	18-25	20-28	20-23	20	19

cidence ($\mu_\theta=0$), only the narrowest distributions ($\sigma_\theta=2,4,6$) exhibited slopes greater than that indicative of areal dependence (Table V and Fig. 5). Therefore, the larger slopes observed in the first set of behavioral simulations at $\mu_\theta=0$ and $\sigma_\theta=8, 10, 20, 40,$ and 60 were due to the choice of ka spacing (Table III). For orientation distributions with large mean tilt angles ($\mu_\theta=80$) and small standard deviations ($\sigma_\theta=2, 4, 6, 8,$ or 10), behavior also had an appreciable effect (Fig. 5). For the distribution of tilt angles $N(80,10)$, the behavior of the target alone was capable of producing slopes close to 30 (indicative of volumetric dependence).

III. SUMMARY

The fits of various scattering models to TS measurements of individual zooplankton were evaluated. The slopes of linear regression lines for TS versus the log of $ka, L, WW,$ and DW indicated that TS is dependent on the cross-sectional area of the animals. This result supports an areally dependent bent-cylinder model for scattering from elongated crustacean zooplankton. This outcome is also in agreement with analyses of encaged aggregations of live zooplankton (Chu *et al.*, 1993) and measurements of individual zooplankton made *in situ* (Demer and Hewitt, submitted). This conclusion appears contradictory to the result from a similar study (Wiebe *et al.*, 1990) in which both the regressions and the best-fit model (HPBC) indicated volumetric dependence. However, neither Wiebe *et al.* (1990) nor the regressions presented in this paper account directly for animal behavior. Furthermore, because the ray BC model of TS vs ka is oscillatory, the linear regression analyses are highly dependent on the range and spacing of the ka 's used.

The apparent discrepancy between these two studies has been explained through simulations that accounted for animal behavior and the range and spacing of ka values used in the analyses. The DWBA model predicts that TS can be dependent on animal volume or cross-sectional area, depending on the distribution of animal orientations. Moreover, linear regression analyses of the ray BC model can predict a large range of slopes which include those indicative of areal and volumetric dependence.

IV. DISCUSSION

Accurate scattering models of zooplankton are necessary for quantitative remote sensing studies using echo sounders. Once corroborated, such predictors can be utilized for one or more purposes including biomass estimation, animal size classification, identification, and delineation of signals from different species, and behavioral observation. Therefore further investigation into the scattering characteristics of specific zooplankton is warranted to better understand the frequency dependence of TS for different classes of scatterers.

To correctly interpret the results of experiments designed to measure the frequency dependence of TS, it is important to consider the basic physics of the scattering of acoustic energy from zooplankton. For elongated animals modeled as bent cylinders, the reduced TS varies with frequency as shown by the ray BC model in Fig. 2. The location of the data points on this curve can affect the interpretation

of the results significantly. At very low frequencies ($ka \ll 1$), the acoustic wavelength is much bigger than the size of the animal and the resulting scatter is omnidirectional. At high frequencies ($ka \gg 1$), the scattering can be described as the interference between two rays, one reflecting from the front interface of the animal and the other from the back interface. In this range of ka there is a Fresnel zone effect (Stanton, 1989a), resulting in deep nulls in the TS vs ka curve (Chu *et al.*, 1992). In addition, at $ka > 1$, the effective cylindrical cross-sectional area changes as a function of animal orientation, making TS sensitive to animal behavior.

For data located in the Rayleigh and transition regions, the slope of a TS vs $\log(ka)$ regression line will be about 40. However, for data in the geometric region, the range and location of ka 's relative to the nulls or the peaks will define the regression slope. Finally, the effects of animal behavior cannot be neglected, as demonstrated in the DWBA simulation results. Changes in both the mean and standard deviation of a target's tilt angle can yield a wide range of regression slopes, ranging from ~ 20 to ~ 30 .

In light of these issues, the use of linear regressions to characterize the dependence of zooplankton TS on acoustic frequency and animal size can yield misleading results and are therefore inappropriate. Rather, analyses of this kind must take into consideration the fundamental physical basis for acoustic scattering from zooplankton. Furthermore, corroboration of theoretical models should also include direct measurements of animal orientations as well as size and impedance contrast.

ACKNOWLEDGMENTS

The enclosure experiment was conducted as part of a Bioacoustical Oceanography workshop at FHL. We wish to thank Gideon Gal, Amatzia Genin, Stein Kaartvedt, Duncan McGehee, and Claudio Richter for their help with the acoustic data collection, Charles Greene for organizing the workshop, and the Office of Naval Research (ONR) for the grant (N00014-93-I-0560). For supplying the echosounding equipment and aiding in the reduction of recorded TS data, we are grateful to Jim Dawson of BioSonics, Inc., and both Tracey Steig and Kevin Kumagai of Hydroacoustic Technology, Inc. Thanks go to our academic advisors, Roger Hewitt, William Hodgkiss, Tim Stanton, and especially Peter Wiebe who helped with the experimental setup and provided spiritual guidance. We are appreciative of Ken Raymond for drawing the experimental setup and Dezhong Chu for supplying helpful comments and the computer code for the DWBA model. Furthermore, DAD would like to thank the John and Fannie Hertz Foundation and LVM would like to thank the Woods Hole Oceanographic Institution/Massachusetts Institute of Technology Joint Program Education Office and ONR Grant No. N00014-92-J-1527 for funding.

Anderson, V. C. (1950). "Sound scattered from a fluid sphere." *J. Acoust. Soc. Am.* 22, 426-431.

Chu, D., Stanton, T. K., and Wiebe P. H. (1992). "Frequency dependence of sound backscattering from live individual zooplankton." *ICES J. Mar. Sci.* 49, 97-106.

- Chu, D., Foote, K. G., and Stanton, T. K. (1993). "Further analysis of target strength measurements of Antarctic krill at 38 and 120 kHz: Comparison with deformed cylinder model and inference of orientation distribution," *J. Acoust. Soc. Am.* **93**, 2985–2988.
- Demer, D. A., and Hewitt, R. P. (submitted). "*In situ* target strength measurements of Antarctic zooplankton (*Euphausia superba* and *Salpa thompsoni*) at 120 and 200 kHz, corroboration of scattering models, and a statistical technique for delineating species," *J. Acoust. Soc. Am.*
- Foote, K. G., Everson, I., Watkins, J. L., and Bone, D. G. (1990). "Target strengths of Antarctic krill (*Euphausia superba*) at 38 and 120 kHz," *J. Acoust. Soc. Am.* **87**, 16–24.
- Foote, K. G. (1990). "Speed of sound in *Euphausia superba*," *J. Acoust. Soc. Am.* **87**, 1405–1408.
- Foote, K. G. (1991). "Summary of methods for determining fish target strength at ultrasonic frequencies," *ICES J. Mar. Sci.* **48**, 211–217.
- Foote, K. G., Chu, D., and Stanton, T. K. (1992). "Status of krill target strength," *CCAMLR Selected Scientific Papers*, pp. 101–126.
- Greene, C. H., Stanton, T. K., Wiebe, P. H., and McClatchie, S. (1991). "Acoustic estimates of Antarctic krill," *Nature* **349**, 110.
- Greenlaw (1977). "Backscattering spectra of preserved zooplankton," *J. Acoust. Soc. Am.* **62**, 44–52.
- Greenlaw, C. F. (1979). "Acoustical estimation of zooplankton populations," *Limnol. Oceanogr.* **24**, 226–242.
- Hewitt, R. P., and Demer, D. A. (1991). "Krill abundance," *Nature* **353**, 310.
- Holliday, D. V., Pieper, R. E., and Kleppel, G. S. (1989). "Determination of zooplankton size and distribution with multi-frequency acoustic technology," *J. Cons. Int. Explor. Mer.* **46**, 52–61.
- Richter, K. E. (1985). "Acoustic scattering at 1.2 MHz from individual zooplankters and copepod populations," *Deep-Sea Res.* **32**, 149–161.
- Stanton, T. K. (1989a). "Sound scattering by cylinders of finite length. III. Deformed cylinders," *J. Acoust. Soc. Am.* **86**, 691–705.
- Stanton, T. K. (1989b). "Simple approximate formulas for backscattering of sound by spherical and elongated objects," *J. Acoust. Soc. Am.* **86**, 691–705.
- Stanton, T. K., Clay, C. S., and Chu, D. (1993a). "Ray representation of sound scattering by weakly scattering deformed fluid cylinders: Simple physics and application to zooplankton," *J. Acoust. Soc. Am.* **94**, 3454–3462.
- Stanton, T. K., Chu, D., Wiebe, P. H., and Clay, C. S. (1993b). "Average echoes from randomly oriented random-length finite cylinders: Zooplankton models," *J. Acoust. Soc. Am.* **94**, 3463–3472.
- Stanton, T. K., Wiebe, P. H., Chu, D., Benfield, M. C., Scanlon, L., Martin, L. V., and Eastwood, R. L. (1994). "On acoustic estimates of zooplankton biomass," *ICES, J. Mar. Sci.* **51**, 505–512.
- Wiebe, P. H., Greene, C. H., Stanton, T. K., and Burczynski, J. (1990). "Sound scattering by live zooplankton and micronekton: Empirical studies with a dual-beam acoustical system," *J. Acoust. Soc. Am.* **88**, 2346–2360.